

## Obstacle Avoidance Control for Redundant Manipulators Using Collidability Measure

Su Il Choi and Byung Kook Kim

Department of Electrical Engineering  
Korea Advanced Institute of Science and Technology  
373-1 Kusong-dong, Yusong-gu, Taejon 305-701 Korea  
E-mail: sichoi@rtcl.kaist.ac.kr, bkkim@ee.kaist.ac.kr

### Abstract

We present a new measure called *collidability measure* for obstacle avoidance control of redundant manipulators. Considering moving directions of manipulator links, the collidability measure is defined as the inverse of sum of predicted collision distances between links and obstacles. This measure is suitable for obstacle avoidance control since directions of moving links are as important as distances to obstacles. For dynamic redundancy resolution, null space control is utilized to avoid obstacles by minimizing the collidability measure. Also, by clarifying decomposition in the joint acceleration level, we present a simple *dynamic* control law with bounded joint torques which guarantees tracking of a given end-effector trajectory and improves a kinematic cost function such as collidability measure. Simulation results are presented to illustrate the effectiveness of the proposed algorithm.

### 1 Introduction

A robot manipulator is defined as *redundant* if it possesses more degrees of freedom than are required to achieve the desired position and orientation of the end-effector. The redundancy of such manipulators can be effectively used to keep within joint limits [1][2], to avoid singularities [3], and to optimize various performance criteria. Also, we can utilize redundancy to avoid obstacles in workspace [4]-[9].

For on-line obstacle avoidance control, many algorithms have been proposed based on pseudoinverse matrix [4]-[6]. Baillieul [7] proposed the *extended Jacobian technique* for solving the inverse kinematics problem, and applied this technique to obstacle avoidance for a class of planar robots and obstacles. In

Khatib's approach [8], redundant robots are controlled directly in Cartesian space using a model-based control law, and obstacle avoidance is achieved using an artificial potential field concept. An important feature of this work is the use of simple geometric "primitives" for representing obstacles. However, the selection of representative points on manipulator links is not simple and the distance value doesn't mean the minimum distance between link and obstacle. Rahmanian-Shahri and Troch [9] presented a new method for on-line collision recognition for robot manipulators. For every link and every obstacle in the workspace, a boundary ellipse is defined such that there is no collision if the robot joints are outside these ellipses.

Many of the above mentioned redundancy resolution approaches require potential function of distances between manipulator and obstacles. Most of the methods assumed that the necessary distance information was given from a higher control level or could be obtained from sensory devices. Gilbert, Johnson, and Keerthi [10] developed an algorithm for computing the Euclidean distance between a pair of convex polytopes. However, suggested distance algorithm is very complex. In all cases, obstacle avoidance control is acted even when manipulator links move away from obstacles. We are going to remedy this problem by considering moving directions of manipulator links with respect to obstacles.

In this paper, We present a new measure called *collidability measure* for obstacle avoidance control of redundant manipulators. Using the collidability measure, we can reduce the magnitude of obstacle avoidance action considerably, especially when manipulator links move away from obstacles. Also, by clarifying decomposition in the joint acceleration level, we present a simple *dynamic* control law with bounded joint torques which guarantees tracking of a given end-

effector trajectory while performing a subtask such as decreasing collidability measure.

This paper is constructed as follows. In Section 2, *collidability measure* is defined and derived. In Section 3, dynamic obstacle avoidance control algorithm is developed. Simulation results are presented in Section 4 to illustrate the performance of the proposed algorithm. This paper ends with concluding remarks in Section 5.

## 2 Collidability Measure

Consider a redundant manipulator with  $n$  degrees of freedom in  $m$  dimensional workspace ( $n > m$ ). The forward kinematics and differential kinematics of the manipulator can be represented as

$$\mathbf{x}_e = \mathbf{f}(\boldsymbol{\theta}) \quad (1)$$

$$\dot{\mathbf{x}}_e = J(\boldsymbol{\theta})\dot{\boldsymbol{\theta}} \quad (2)$$

where  $\mathbf{x}_e \in R^m$  represents position and orientation of the end-effector,  $\boldsymbol{\theta} \in R^n$  represents joint variables,  $\mathbf{f}(\boldsymbol{\theta}) \in R^m$  is a vector function describing the manipulator kinematics, and  $J(\boldsymbol{\theta}) \in R^{m \times n}$  is the end-effector Jacobian matrix. The general solution of Eq. (2) is

$$\dot{\boldsymbol{\theta}} = J^+ \dot{\mathbf{x}}_e + (I - J^+ J)\mathbf{g} \quad (3)$$

where  $J^+ = J^T(JJ^T)^{-1}$  is the pseudoinverse of  $J$ ,  $I \in R^{n \times n}$  is the identity matrix, and  $\mathbf{g} \in R^n$  is an arbitrary vector in the joint-velocity space which can be used to resolve the redundancy at the velocity level in optimizing a suitable performance criterion.

We use  $\mathcal{A}$  and  $\mathcal{O}$  to denote the manipulator links and obstacles respectively. The manipulator and obstacles are represented by unions of objects as follows:

$$\mathcal{A} = \bigcup_{i \in I_{\mathcal{A}}} \mathcal{A}_i, \quad \mathcal{O} = \bigcup_{j \in I_{\mathcal{O}}} \mathcal{O}_j \quad (4)$$

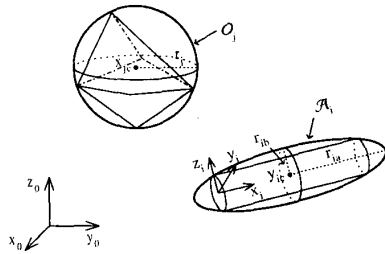


Figure 1: Link object  $\mathcal{A}_i$  and obstacle object  $\mathcal{O}_j$ .

where  $\mathcal{A}_i, i \in I_{\mathcal{A}} = \{1, \dots, n\}$  are manipulator links, and  $\mathcal{O}_j, j \in I_{\mathcal{O}} = \{1, \dots, n_{\mathcal{O}}\}$  are  $n_{\mathcal{O}}$  obstacles. Consider a link-obstacle pair as shown in Fig. 1. The problem is to determine a joint trajectory  $\boldsymbol{\theta}(t)$  of the manipulator so that its end-effector can move along the desired trajectory while the manipulator  $\mathcal{A}$  is kept away from obstacles  $\mathcal{O}$ . Link  $\mathcal{A}_i$  is assumed to be a cylinder, which can be described as an ellipsoid containing the link centered at  $\mathbf{y}_{ic}$  in the link  $i$  coordinate frame described as [11]

$$\mathcal{A}_i(\boldsymbol{\theta}) = \{T_i(\boldsymbol{\theta})\mathbf{y} : (\mathbf{y} - \mathbf{y}_{ic})^T Q_i^T Q_i (\mathbf{y} - \mathbf{y}_{ic}) \leq 1\} \quad (5)$$

with

$$Q_i = \begin{bmatrix} 1/r_{ia} & 0 & 0 \\ 0 & 1/r_{ib} & 0 \\ 0 & 0 & 1/r_{ib} \end{bmatrix} \quad (6)$$

where  $r_{ia}$  and  $r_{ib}$  are scalar coefficients, and  $T_i(\boldsymbol{\theta})$  is a homogeneous transformation matrix for link  $i$  coordinate frame which consists of an orthogonal rotation matrix  $R_i(\boldsymbol{\theta})$  and a position vector  $\mathbf{p}_i(\boldsymbol{\theta})$  [12]:

$$T_i(\boldsymbol{\theta}) = \begin{bmatrix} R_i(\boldsymbol{\theta}) & \mathbf{p}_i(\boldsymbol{\theta}) \\ 0 & 0 & 0 & 1 \end{bmatrix} \quad (7)$$

Obstacle  $\mathcal{O}_j$  is assumed to be a general convex shape, which can be described as a spherical object containing the obstacle with radius  $r_j$  centered at  $\mathbf{x}_{jc}$  described as

$$\mathcal{O}_j = \{\mathbf{x} : (\mathbf{x} - \mathbf{x}_{jc})^T S_j^T S_j (\mathbf{x} - \mathbf{x}_{jc}) \leq 1\} \quad (8)$$

where

$$S_j = \begin{bmatrix} 1/r_j & 0 & 0 \\ 0 & 1/r_j & 0 \\ 0 & 0 & 1/r_j \end{bmatrix} \quad (9)$$

In order to determine a unique solution of Eq. (3), an additional condition should be introduced, such as minimization of a performance index. Hence, we introduce a new performance measure called *collidability measure* for obstacle avoidance considering moving directions of manipulator links and obstacles, which is defined as the inverse of sum of predicted collision distances between links and obstacles.

Consider now the problem of finding the collidability measure of the link  $i$  and the obstacle  $j$ . For simplicity of detecting collision between them, elliptical link  $\mathcal{A}_i$  and spherical obstacle  $\mathcal{O}_j$  are viewed as expanded elliptical link  $\hat{\mathcal{A}}_i$  and shrunk point obstacle  $\hat{\mathcal{O}}_j$ , as shown in Fig. 2(a):

$$\hat{\mathcal{A}}_i = \{\mathbf{x} : (\mathbf{x} - \mathbf{x}_{ic})^T Q^T Q (\mathbf{x} - \mathbf{x}_{ic}) \leq 1\} \quad (10)$$

$$\hat{\mathcal{O}}_j = \{\mathbf{x} : \mathbf{x} = \mathbf{x}_{jc}\} \quad (11)$$

where  $\mathbf{x}_{ic} = T_i(\boldsymbol{\theta})\mathbf{y}_{ic}$ , and  $Q = (Q_i^{-1} + S_j^{-1})^{-1}R_i^T$ . Next, define  $\mathbf{x}_c$  as relative position between  $\mathbf{x}_{jc}$  and  $\mathbf{x}_{ic}$

$$\mathbf{x}_c = \mathbf{x}_{jc} - \mathbf{x}_{ic}. \quad (12)$$

We assume that instantaneous movement of  $\mathbf{x}_c$  at time  $t$  is maintained during  $[t, t + \tau]$  for small  $\tau$ . Then, the predicted motion of  $\mathbf{x}_c$  for primary task (tracking any arbitrary trajectory) is represented as follows:

$$\mathbf{x}_c(t + \tau) = \mathbf{x}_c(t) + \mathbf{v}_c(t)\tau \quad (13)$$

$$\mathbf{v}_c(t) = \dot{\mathbf{x}}_{jc} - \left(\frac{\partial T_i(\boldsymbol{\theta})}{\partial \boldsymbol{\theta}} \dot{\boldsymbol{\theta}}_d(t)\right) \mathbf{y}_{ic} \quad (14)$$

with

$$\dot{\boldsymbol{\theta}}_d(t) = J^+(\boldsymbol{\theta})\dot{\mathbf{x}}_d(t) \quad (15)$$

where  $\mathbf{v}_c(t)$  is the velocity of  $\mathbf{x}_c(t)$ ,  $\dot{\boldsymbol{\theta}}_d(t)$  is a desired joint velocity,  $\dot{\mathbf{x}}_d(t)$  is a desired end-effector velocity.

Elliptical link  $\hat{A}_i$  will collide with point obstacle  $\hat{O}_j$  if the following conditions are satisfied.

$$\begin{aligned} \mathbf{v}_c^T Q^T Q \mathbf{x}_c &< 0, \\ (\mathbf{v}_c^T Q^T Q \mathbf{x}_c)^2 - |Q \mathbf{v}_c|^2 (|Q \mathbf{x}_c|^2 - 1) &\geq 0. \end{aligned} \quad (16)$$

The predicted collision time  $t_p$  is obtained by solving

$$(\mathbf{x}_c + t_p \mathbf{v}_c)^T Q^T Q (\mathbf{x}_c + t_p \mathbf{v}_c) = 1. \quad (17)$$

Then, the predicted collision time  $t_p$  and the predicted collision point  $\mathbf{x}_p$  are obtained as

$$\begin{aligned} |Q \mathbf{v}_c|^2 t_p &= -(\mathbf{v}_c^T Q^T Q \mathbf{x}_c) \\ &\quad - \sqrt{(\mathbf{v}_c^T Q^T Q \mathbf{x}_c)^2 - |Q \mathbf{v}_c|^2 (|Q \mathbf{x}_c|^2 - 1)} \quad (18) \\ \mathbf{x}_p &= \mathbf{x}_c + t_p \mathbf{v}_c. \end{aligned} \quad (19)$$

Using the predicted collision point  $\mathbf{x}_p \in \hat{A}_i$ , predicted collision points  $\mathbf{x}_{ip} \in \mathcal{A}_i$  and  $\mathbf{x}_{jp} \in \mathcal{O}_j$  are obtained as

$$\mathbf{x}_{ip} = \mathbf{x}_{ic} + R_i Q_i^{-1} Q \mathbf{x}_p \quad (20)$$

$$\mathbf{x}_{jp} = \mathbf{x}_{jc} + (R_i Q_i^{-1} Q - I) \mathbf{x}_p. \quad (21)$$

Basically, the collidability measure  $c_{ij}(\boldsymbol{\theta})$  is defined as the inverse of the predicted collision distance  $|\mathbf{x}_{ip} - \mathbf{x}_{jp}|$ . In case Eq. (16) is not satisfied, collision will not happen. To make smooth variation of  $c_{ij}(\boldsymbol{\theta})$  beyond the collision region, we assume the velocity vector  $\mathbf{v}_b$ , obtained by rotating  $\mathbf{v}_c$  to the origin, makes collision between  $\hat{O}_j$  and the boundary point of  $\hat{A}_i$ . As shown in Fig. 2(b), by counterclockwise rotation of  $\mathbf{v}_c$  with

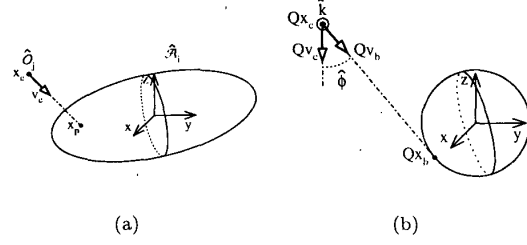


Figure 2: Collision between  $\hat{A}_i$  and  $\hat{O}_j$  (a) Predicted collision point  $\mathbf{x}_p$  and (b) Boundary collision point  $\mathbf{x}_b$ .

respect to the vector  $\hat{\mathbf{k}}$ ,  $\mathbf{v}_b$  can be obtained as follows:

$$\hat{\mathbf{k}} = \frac{(Q \mathbf{v}_c) \times (-Q \mathbf{x}_c)}{|(Q \mathbf{v}_c) \times (-Q \mathbf{x}_c)|} \quad (22)$$

$$\begin{aligned} \hat{\phi} &= \cos^{-1} \left( \frac{(Q \mathbf{v}_c) \cdot (-Q \mathbf{x}_c)}{|Q \mathbf{v}_c| |Q \mathbf{x}_c|} \right) \\ &\quad - \cos^{-1} \left( \frac{\sqrt{|Q \mathbf{x}_c|^2 - 1}}{|Q \mathbf{x}_c|} \right) \end{aligned} \quad (23)$$

$$\mathbf{v}_b = Q^{-1} R_{\hat{\mathbf{k}}}(\hat{\phi}) Q \mathbf{v}_c \quad (24)$$

where  $\hat{\phi}$  is the angle difference between  $Q \mathbf{v}_c$  and  $Q \mathbf{v}_b$ , and  $R_{\hat{\mathbf{k}}}$  is the rotation matrix. Given the velocity  $\mathbf{v}_b$ , the boundary collision time  $t_b$  and the boundary collision point  $\mathbf{x}_b$  on the elliptical link  $\hat{A}_i$  are obtained as

$$t_b = \frac{(Q \mathbf{v}_b) \cdot (-Q \mathbf{x}_c)}{|Q \mathbf{v}_b|^2} = \frac{\sqrt{|Q \mathbf{x}_c|^2 - 1}}{|Q \mathbf{v}_c|} \quad (25)$$

$$\mathbf{x}_b = \mathbf{x}_c + t_b \mathbf{v}_b. \quad (26)$$

Using the boundary collision point  $\mathbf{x}_b \in \hat{A}_i$ , boundary collision points  $\mathbf{x}_{ib} \in \mathcal{A}_i$  and  $\mathbf{x}_{jb} \in \mathcal{O}_j$  are obtained as

$$\mathbf{x}_{ib} = \mathbf{x}_{ic} + R_i Q_i^{-1} Q \mathbf{x}_b \quad (27)$$

$$\mathbf{x}_{jb} = \mathbf{x}_{jc} + (R_i Q_i^{-1} Q - I) \mathbf{x}_b. \quad (28)$$

Then, the angle difference between  $\mathbf{v}_c$  and  $(\mathbf{x}_{ib} - \mathbf{x}_{jb})$  is obtained as

$$\phi = \cos^{-1} \left( \frac{\mathbf{v}_c \cdot (\mathbf{x}_{ib} - \mathbf{x}_{jb})}{|\mathbf{v}_c| |\mathbf{x}_{ib} - \mathbf{x}_{jb}|} \right) \quad (29)$$

Next, a cubic polynomial of the form

$$g(\phi) = a_0 + a_1 \phi + a_2 \phi^2 + a_3 \phi^3 \quad (30)$$

defined in  $0 \leq \phi \leq \phi_{max}$ , where  $\phi_{max}$  represents the angular spline interval, can be splined to fit four

boundary conditions of

$$\begin{aligned} g(0) &= \frac{1}{|\mathbf{x}_{ib} - \mathbf{x}_{jb}|} \\ \dot{g}(0) &= \frac{-1}{|\mathbf{x}_{ib} - \mathbf{x}_{jb}|^2} \frac{d|\mathbf{x}_{ib} - \mathbf{x}_{jb}|}{d\phi} \\ g(\phi_{max}) &= 0 \\ \dot{g}(\phi_{max}) &= 0. \end{aligned} \quad (31)$$

The resultant cubic polynomial is

$$\begin{aligned} g(\phi) &= g(0) + \dot{g}(0)\phi - \frac{1}{\phi_{max}^2} (3g(0) + 2\dot{g}(0)\phi_{max})\phi^2 \\ &+ \frac{1}{\phi_{max}^3} (2g(0) + \dot{g}(0)\phi_{max})\phi^3. \end{aligned} \quad (32)$$

Finally, we can get the collidability measure  $c_{ij}(\boldsymbol{\theta})$  of the link  $i$  and the obstacle  $j$  as

$$c_{ij}(\boldsymbol{\theta}) = \begin{cases} \frac{1}{|\mathbf{x}_{ip} - \mathbf{x}_{jp}|} & \text{if Eq. (16) is satisfied} \\ g(\phi) & \text{if } 0 \leq \phi \leq \phi_{max} \\ 0 & \text{if } \phi > \phi_{max}. \end{cases} \quad (33)$$

The collidability measure between the manipulator and obstacles is obtained as

$$C(\boldsymbol{\theta}) = \sum_{i \in I_A, j \in I_O} c_{ij}(\boldsymbol{\theta}) \quad (34)$$

### 3 Obstacle Avoidance Control

In this section, we derive a new dynamic redundancy control algorithm considering joint torque saturation. Differentiating Eq. (2), we obtain the differential relation between the end-effector acceleration and the joint acceleration

$$\ddot{\mathbf{x}}_e = J\ddot{\boldsymbol{\theta}} + \dot{J}\dot{\boldsymbol{\theta}}. \quad (35)$$

The general solution of Eq. (35) can be obtained using pseudoinverse as

$$\ddot{\boldsymbol{\theta}} = J^+(\ddot{\mathbf{x}}_e - \dot{J}\dot{\boldsymbol{\theta}}) + \ddot{\boldsymbol{\theta}}_N \quad (36)$$

where  $\ddot{\boldsymbol{\theta}}_N = (I - J^+J)\mathbf{h}$  is a vector in the null space of  $J$ , and  $\mathbf{h} \in R^n$  is an arbitrary vector in the joint acceleration space.

Consider the case where the solution of joint velocity is given as Eq. (3) with an arbitrary vector  $\mathbf{g} \in R^n$  and we want to obtain the solution of joint acceleration. Differentiating Eq. (3), we obtain the differential Eq. (36) and some relations between them.

**Proposition 1** *Let's decompose  $\ddot{\boldsymbol{\theta}}$  into range space component  $\ddot{\boldsymbol{\theta}}_R = J^+(\ddot{\mathbf{x}}_e - \dot{J}\dot{\boldsymbol{\theta}})$  and null space component  $\ddot{\boldsymbol{\theta}}_N = (I - J^+J)\mathbf{h}$ . Then*

$$\ddot{\boldsymbol{\theta}}_R = \left(\frac{d\dot{\boldsymbol{\theta}}_R}{dt}\right)_R + \left(\frac{d\dot{\boldsymbol{\theta}}_N}{dt}\right)_R \quad (37)$$

$$\ddot{\boldsymbol{\theta}}_N = \left(\frac{d\dot{\boldsymbol{\theta}}_R}{dt}\right)_N + \left(\frac{d\dot{\boldsymbol{\theta}}_N}{dt}\right)_N \quad (38)$$

$$\mathbf{h} = \dot{\mathbf{g}} + (J^+J)^T(\dot{\boldsymbol{\theta}}_R - \mathbf{g}). \quad (39)$$

By using  $J^+ = (I - J^+J)j^T(JJ^T)^{-1} - J^+JJ^+$  (see Ma and Hirose [14]), proving of proposition 1 is simple.

The general form of manipulator dynamics is given by

$$M(\boldsymbol{\theta})\ddot{\boldsymbol{\theta}} + N(\boldsymbol{\theta}, \dot{\boldsymbol{\theta}}) = \boldsymbol{\tau} \quad (40)$$

where  $M(\boldsymbol{\theta}) \in R^{n \times n}$  is a symmetric, positive definite inertia matrix,  $N(\boldsymbol{\theta}, \dot{\boldsymbol{\theta}}) \in R^n$  is a vector containing nonlinear terms such as Coriolis, centrifugal, and gravitational forces, and  $\boldsymbol{\tau} \in R^n$  is a vector of joint actuating torques. Given a desired trajectory,  $\mathbf{x}_d(\cdot)$ , we want to choose  $\boldsymbol{\tau}$  so that the actual trajectory tracks the desired one, as well as achieving a subtask.

A dynamic control law to track a given workspace trajectory is obtained using Eqs. (36) and (40):

$$\boldsymbol{\tau} = M \left\{ J^+(\ddot{\mathbf{x}}_d + K_v\dot{\mathbf{e}} + K_p\mathbf{e} - \dot{J}\dot{\boldsymbol{\theta}}) + \phi_N \right\} + N \quad (41)$$

where  $\mathbf{e} \triangleq \mathbf{x}_d - \mathbf{x}_e$  is the tracking error,  $K_v$  and  $K_p$  are constant feedback gain matrices, and  $\phi_N$  is any vector in the null space of  $J$ . If the manipulator does not go through a singularity, then the control law Eq. (41) guarantees that the tracking error converges to zero[13].

Next, consider the case where we are given a vector function  $\mathbf{g} = \alpha \nabla C(\boldsymbol{\theta}) \in R^n$  for obstacle avoidance and we want the null space joint velocity to track the projection of  $\mathbf{g}$  onto the null space of  $J$ , where  $\alpha$  is a gain constant. Since  $(I - J^+J)$  projects vectors onto the null space of  $J$ , this is the same as asking that

$$\dot{\mathbf{e}}_N \triangleq (I - J^+J)\dot{\mathbf{g}} - \dot{\boldsymbol{\theta}}_N \quad (42)$$

converge to zero. The following proposition shows how to choose  $\phi_N$  to get the desired result.

**Proposition 2** *Assume that the manipulator does not go through a singularity. Let the control be given by Eq. (41) with*

$$\phi_N = (I - J^+J)\{\dot{\mathbf{g}} + (J^+J)^T(\dot{\boldsymbol{\theta}}_R - \mathbf{g}) + K_N\dot{\mathbf{e}}_N\} \quad (43)$$

where  $K_N$  is a positive definite feedback matrix. Then the tracking error  $\mathbf{e}$  converges to zero and the joint velocity converges to  $\mathbf{g}$  in the null space of  $J$ , i.e.,  $\dot{\mathbf{e}}_N \rightarrow 0$ .

Let the joint torque is bounded by

$$|\tau_i| \leq \tau_{i,max}, \quad i \in I_A \quad (44)$$

where  $\tau_{i,max}$  is the upper limit of each joint torque. Decompose  $\boldsymbol{\tau}$  as  $\boldsymbol{\tau} = \boldsymbol{\tau}_R + \boldsymbol{\tau}_N$  where

$$\begin{aligned} \boldsymbol{\tau}_R &= M J^+ (\ddot{\mathbf{x}}_d + K_v \dot{\mathbf{e}} + K_p \mathbf{e} - \dot{J} \dot{\boldsymbol{\theta}}) + N \\ \boldsymbol{\tau}_N &= M \boldsymbol{\phi}_N \end{aligned} \quad (45)$$

In some cases, excessively large null space joint torque  $\boldsymbol{\tau}_N$  is required to achieve the given subtask. To prevent such a case, we utilize a saturation function as follows.

**Proposition 3** Define a torque saturation function as

$$\text{Sat}(\boldsymbol{\tau}_N) = \min(1, \alpha_\tau) \boldsymbol{\tau}_N \quad (46)$$

where

$$\alpha_\tau = \min_{(\tau_N)_i \neq 0, i=1, \dots, n} \frac{\text{sgn}((\tau_N)_i) \tau_{i,max} - (\tau_R)_i}{(\tau_N)_i} \quad (47)$$

Then, each component of the joint torque  $\boldsymbol{\tau} = \boldsymbol{\tau}_R + \text{Sat}(\boldsymbol{\tau}_N)$  satisfies the torque bound  $\tau_{i,max}$ .

The purpose of this dynamic control law is to make the self-motion or the null space joint velocity  $\dot{\boldsymbol{\theta}}_N = (I - J^+ J) \dot{\boldsymbol{\theta}}$  track the projection of  $\mathbf{g}$  on the null space of  $J$ , which is the same as asking that  $\dot{\mathbf{e}}_N$  should converge to zero. This dynamic control law permits end-effector trajectory tracking while decreasing the possibility of collision via minimizing the collidability measure.

## 4 Simulation

Consider a four-link manipulator moving in three dimensional space with two spherical obstacles. We choose parameters as follows: Link lengths  $l_i = 1 \text{ m}$ ,  $i = 1, \dots, 4$ ; link masses  $m_i = 10 \text{ kg}$ ,  $i = 1, \dots, 4$ ; inertia parameters  $I_i = 5/6 \text{ kgm}^2$ ,  $i = 1, \dots, 4$ .

For dynamic obstacle avoidance control, simulation is done with the desired trajectory, which is given as a straight line Cartesian path starting and ending with

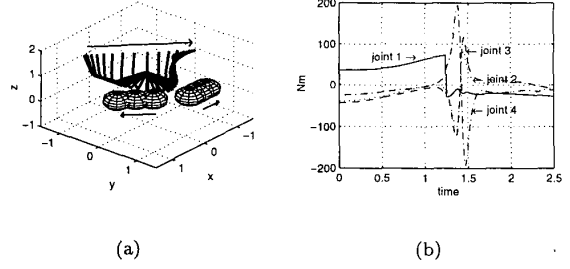


Figure 3: Kinematic obstacle avoidance control with collidability measure (a) Trajectories, (b) Joint velocities.

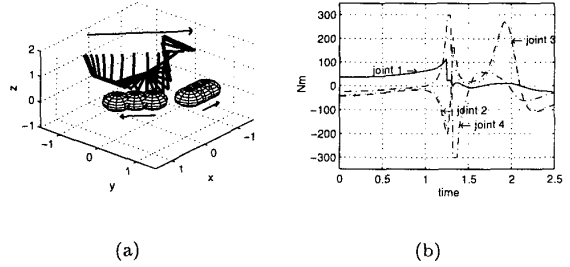


Figure 4: Kinematic obstacle avoidance control with conventional measure (a) Trajectories, (b) Joint velocities.

zero velocity, with constant bang-bang type acceleration/deceleration  $\ddot{\mathbf{x}}_d = [-1 \ 1 \ 0]^T \text{ m/sec}^2$ . We choose  $\mathbf{g} = \alpha_1 \nabla C + \alpha_2 \nabla H$  to minimize the collidability measure  $C(\boldsymbol{\theta})$  and maximize the manipulability measure  $H(\boldsymbol{\theta}) = \sqrt{\det(JJ^T)}$ , where  $\alpha_1 = -0.292$  and  $\alpha_2 = 0.1$  are gain constants. Two spherical obstacles do uniform motion, and the joint torque bound  $\tau_{i,max} = 300 \text{ Nm}$ ,  $i = 1, \dots, 4$ . Using dynamic control algorithm with the collidability measure, Fig. 3(a) shows the resultant trajectory with moving obstacles. Joint torques are shown in Fig. 3(b).

For comparison, obstacle avoidance control with a conventional measure – inverse of minimum distance – is simulated. In this case, Fig. 4(a) shows the resultant trajectory with moving obstacles. Joint torques are shown in Fig. 4(b). Fig. 5 shows that obstacle avoidance control with the collidability measure is economic, since it requires much less joint torque than the conventional measure.

Some simulations are performed to reveal that our control algorithm with the collidability measure re-

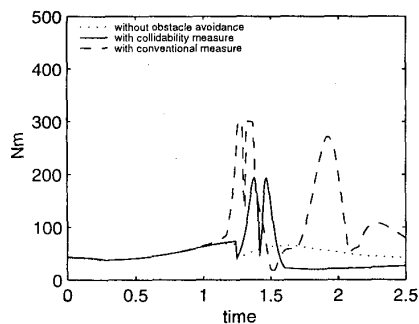


Figure 5: Joint torque norm  $\|\tau\|_\infty$  for three cases.

quires less null space control action for obstacle avoidance, leaving more actions possible for improving other measures such as manipulability measure.

## 5 Conclusion

We presented a new measure called *collidability measure* for obstacle avoidance control of redundant manipulators. Obstacle avoidance action is reduced remarkably, since the collidability measure is obtained based on the relative movements of manipulator links and obstacles, and produces less null space control action. We also presented simple dynamic control law with bounded joint torque which guarantee asymptotic tracking of a desired trajectory while performing desired subtasks. This control law satisfies joint torque bound, and allows reasonably large gain to improve the system performance. Effectiveness of the proposed collidability measure have been demonstrated with some simulations.

## References

- [1] A. Liegeois, "Automatic supervisory control of the configuration and behavior of multi-body mechanisms," *IEEE Trans. on System, Man, and Cybernetics*, vol. 7, no. 12, pp. 868-871, 1977.
- [2] C.A. Klein and C. Huang, "Review of pseudoinverse control for use with kinematically redundant manipulators," *IEEE Trans. on System, Man, and Cybernetics*, vol. 13, no. 3, pp. 245-250, 1983.
- [3] T. Yoshikawa, "Manipulability of robot mechanism," *Int. J. of Robotics Research*, vol. 4, no. 2, pp.3-9, 1985.
- [4] A.A. Maciejewski and C.A. Klein, "Obstacle avoidance for kinematically redundant manipulators in dynamically varying environments," *Int. J. of Robotics Research*, vol. 4, no. 3, pp. 109-117, 1985.
- [5] Y. Nakamura, H. Hanafusa and T. Yoshikawa, "Task-priority based on redundant control of robot manipulators," *Int. J. of Robotics Research*, vol. 6, no. 2, pp. 3-15, 1987.
- [6] M. Kircanski and M. Vukobratovic, "Contribution to control of redundant robotic manipulators in an environment with obstacles," *Int. J. of Robotics Research*, vol. 5, no. 4, pp. 112-119, 1986.
- [7] J. Baillieul, "Avoiding obstacles and resolving kinematic redundancy," *IEEE Int. Conf. on Robotics and Automation*, pp. 1698-1704, 1986.
- [8] O. Khatib, "Real-time obstacle avoidance for manipulators and mobile robots," *Int. J. Rob. Res.*, vol. 5, no. 1, pp. 90-98, 1986.
- [9] N. Rahmanian-Shari and I. Troch, "Collision-avoidance control for redundant articulated robots," *Robotica*, vol. 13, pp. 159-168, 1995.
- [10] E.G. Gilbert, D.W. Johnson, and S.S. Keerthi, "A Fast Procedure for Computing the Distance Between Complex Objects in Three-Dimensional Space," *IEEE J. Robotics and Automation*, vol. 4, no. 2, pp. 193-203, 1988.
- [11] C.J. Wu, "On the Representation and Collision Detection of Robots," *J. of Intelligent and Robotic Systems*, vol. 16, pp. 151-168, 1996.
- [12] K.S. Foo, R.C. Gonzalez, and C.S.G. Lee, *Robotics: Control, Sensing, Vision and Intelligence*. McGraw-Hill, 1987.
- [13] P. Hsu, J. Hauser and S. Sastry, "Dynamic control of redundant manipulators," *J. Robotic Systems*, vol. 6, no. 2, pp. 133-148, 1989.
- [14] S. Ma and S. Hirose, "Dynamic redundancy resolution of redundant manipulators with local optimization of a kinematic criterion," *Proc. 2nd Asian Conf. of Robotics and its Application*, pp.236-243, 1994.